Feature Extraction Method for Palmprint Considering Elimination of Creases

Jun-ichi FUNADA[†] Naoya OHTA[††] Masanori MIZOGUCHI[†] Tsutomu TEMMA[†††]
Kaoru NAKANISHI[‡] Arata MURAI[‡] Toshio SUGIUCHI[‡‡]
Toshio WAKABAYASHI[‡‡] Yoshifumi YAMADA[‡‡‡]
[†]C&C Media Research Laboratories, NEC Corporation
[††]Department of Computer Science, Gunma University [†††]Incubation Center, NEC Corporation
[‡] Information Management Division, Information Communications Bureau, National Police Agency
[‡‡] Identification Division, Criminal Investigation Bureau, National Police Agency
[‡‡‡]Security Electronics & Communications Technology Association
Address: [†] 4-1-1 Miyazaki, Miyamae-ku Kawasaki, 216-8555, Japan
E-mail: funada@ccm.cl.nec.co.jp

Abstract

A new method of extracting palmprint features is presented in this report. Since palmprint images have many creases which are organized like ridges, ordinary fingerprint feature extraction algorithms are unable to extract ridges. Consequently, the goal of this research is to construct a new feature extraction method which can extract ridges under these conditions. At first, the original palmprint image is divided into local images. The ridge candidates are extracted from each local image of the palmprint. Finally, only one candidate is selected as the ridge in the local image by estimating the continuity of certain properties. Experiments with palmprint images indicate that the proposed method can extract ridges better than conventional methods, especially in areas in which both ridges and creases exist.

1. Introduction

Palmprints are the pattern of skin on the surface of the palm. Ridges exist all over the palmprints, as they do in fingerprints. Palmprint patterns can thus be used to identify persons, because they remained unchanged throughout the life of an individual and no two palmprints from different persons are the same. The matching of different fingerprints is achieved by maching the terminations and the bifurcations of the ridges that constitute a fingerprint pattern. These feature points are called "minutiae". There are also minutiae in palmprints and thus matching of different palmprints is also achieved by minutiae maching. In this paper, we propose a new minutiae extraction method for palmprints.

At first glance, fingerprint and palmprint patterns appear to closely resemble each other. Minutiae extraction methods for fingerprints, however are not suitable for palmprints. Various methods for minutiae extraction for fingerprints have been investigated([1][2][3][4][5]). In most of these methods, local ridge orientations are detected and images are enhanced according to the orientation for removal of noise. The enhanced images are then binarized and thinned to obtain minutiae.

When fingerprint feature extraction methods are applied to palmprints, the orientation detection becomes a major problem. This is because methods to detect orientations were designed under the assumption that the flow of the ridges was the only orientational component in the image. Thus, the methods for fingerprints detect the major flow as the fingerprint ridges. In palmprints, however, this assumption is wrong, because creases and ridges overlapp and cross each other. Hence, creases are often detected when fingerprint feature extraction methods are applied to palmprints and the original image is enhanced along the flow of creases. Consequently, restored images contain many creases. Moreover, the local properties of creases and ridges in palmprints resemble each other, and so a feature

extraction method for palmprints needs to have the ability to distinguish creases and ridges by their global properties.

An example palmprint image is shown in Fig.1. In this image, the ridges of the palmprint are the lines which flow from top to bottom of the image. The other lines are creases.

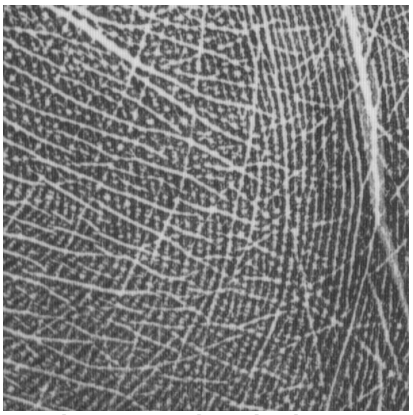

Figure 1. Palmprint image

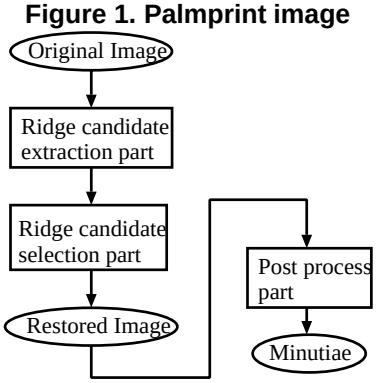

Figure 2. Block diagram of new method

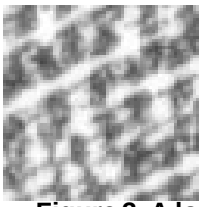

Figure 3. A local image $g^{I_{ij}}(x, y)$

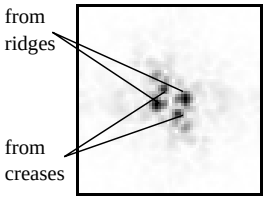

Figure 4. A power spectrum $|H^{I_{ij}}(\xi, \eta)|^2$

Since the palm includes many creases like this, it is difficult to distinguish creases from ridges from their local properties alone, because these properties are very similar. Moreover, the direction and pitch of the creases vary continuously. Accordingly, in discussing the feature extraction methods for palmprint images, the presence of creases must be taken into consideration.

In our new method, several ridge candidates in each local area are initially extracted by fitting the local image to a ridge model. The candidates which according to the model are highly likely to be ridges are then detected. In the next step, the correct candidates (i.e. those which actually are the local ridges) are selected in each of the local areas on the basis of their continuity with the candidates selected in the previous step. Finally, a restored image is constructed by using these detected candidates.

In the next section (Section 2), we introduce the concept of the new method. Section 3 explains the local information extraction process which extracts the candidates from the local images, and Section 4 explains the selection process which selects the candidate corresponding to the ridge in each area. In Section 5 we report experimental results.

2. Overview of the algorithm

The overall block diagram of our new method is shown in Fig.2. The procedure consists of three main parts: ridge candidate extraction part, ridge candidate selection part, and post process part. First a palmprint image is fed to the ridge candidate extraction part. Here, the image is divided into small local area images, and several ridge candidates are detected by using only local information in each local area. Since several candidates are extracted, they include both ridges and creases. Next, in the ridge candidate selection part, the candidates which represent the ridges are selected in each local area by using global information such as the continuity. An image is then constructed by the candidates which are selected in each of the local areas. This restored image does not have noise or creases. Then in the post process part, the image is binarized, thinned, checked for correctability as the thinned image, and repaired. Finally minutiae are extracted from the thinned image. In the post process part, conventional methods[1] are used.

3. Ridge candidate extraction part

In the ridge candidate extraction part, a palmprint image is divided into small local area images, and a plurality of ridge candidates is detected by using only local information in each local area. Since the local ridge pattern of a palmprint can be approximated well by a 2-dimensional sine wave, we propose that the local ridge pattern be modeled by such a wave. Since a 2-d sine wave in the image corresponds to a pair of peaks in its power spectrum, a local image is fitted to the model by detecting peaks in its power spectrum. Moreover, in order to detect a plurality of candidates from an area, a

plurality of peaks is detected. Using this method, even if areas contain both creases and ridges, the ridges and the creases can be separated, with both being detected as ridge. Since candidates from ridges are often the principal ingredient, the peaks are detected in order of their amplitude. The number of peaks detected in this step is predetermined.

The algorithm of this part is as follows. Let the size of the original image be $N_x \times N_y pixel$ and the size of the local area be $M \times Mpixel$. Let I_{ij} be the local area which is located in i-th to the right of and j-th below the top-left local area. For each local area, the candidate extraction is done using the $L \times Lpixel(L > M)$ image of which the local area is located at the center(L is odd). This local image is defined as $g^{I_{ij}}(x,y)(-L/2-1 \leq x,y \leq L/2)$. The window function for Fourier transform, $w(x,y)$, is defined as follows: $w(x,y) \equiv \frac{1}{2\pi\sigma^2}\exp\left(-\frac{x^2+y^2}{2\sigma^2}\right)$. The procedure consists of six stages:

The ridge candidate extraction part:

The following steps are done for the all local areas($\{I_{ij}|0 \leq i \leq N_x/M-1, 0 \leq j \leq N_y/M-1\}$).

Step1. DC component $d_c^{I_{ij}}$ is calculated as follows: $d_c^{I_{ij}} = \sum_{x=-L/2+1}^{L/2}\sum_{y=-L/2+1}^{L/2} w(x,y)g^{I_{ij}}(x,y)$.

Step2. $h^{I_{ij}}(x,y)$ is calculated as follows: $h^{I_{ij}}(x,y) = w(x,y)(g^{I_{ij}}(x,y) - d_c^{I_{ij}})$

Step3. The power spectrum of $h^{I_{ij}}(x,y)$, which is denoted $H^{I_{ij}}(\xi,\eta)$, is calculated.

Step4. K peaks in $|H^{I_{ij}}(\xi,\eta)|^2$ are detected in the order of their amplitude. The search range is $\{(\xi,\eta)|\xi \geq 0, \eta \leq 0 \ or \ \xi > 0, \eta > 0\}$. Let the location of each peaks be $\{(\xi_k^{I_{ij}}, \eta_k^{I_{ij}})\}_{k=1}^K$.

Step5. For each peak, the following features are calculated:

$$\begin{aligned}
amplitude: a_k^{I_{ij}} &= 2|H^{I_{ij}}(\xi_k^{I_{ij}}, \eta_k^{I_{ij}})| \\
phase: ph_k^{I_{ij}} &= \tan^{-1}\left(\frac{Im\{H^{I_{ij}}(\xi_k^{I_{ij}}, \eta_k^{I_{ij}})\}}{Re\{H^{I_{ij}}(\xi_k^{I_{ij}}, \eta_k^{I_{ij}})\}}\right) \\
direction: d_k^{I_{ij}} &= \tan^{-1}(\eta_k^{I_{ij}}/\xi_k^{I_{ij}}) \\
frequency: f_k^{I_{ij}} &= \frac{1}{L}\sqrt{(\xi_k^{I_{ij}})^2 + (\eta_k^{I_{ij}})^2} \\
energy: va_k^{I_{ij}} &= \frac{4\pi^2\sigma^4}{L^2}\sum_{(\xi,\eta)\in D} 2|H^{I_{ij}}(\xi,\eta)|^2 \\
k &= 1,2,\cdots,K
\end{aligned} \tag{1}$$

D is 8-neighbor of (ξ_k, η_k).

Step6. Total energy of $h^{I_{ij}}$ is calculated as follows: $v_T^{I_{ij}} = \frac{4\pi^2\sigma^4}{L^2}\sum_{\xi=-L/2+1}^{L/2}\sum_{\eta=-L/2+1}^{L/2}|H^{I_{ij}}(\xi,\eta)|^2$.

The image which is expressed by the information $a_k^{I_{ij}}, ph_k^{I_{ij}}, d_k^{I_{ij}}, f_k^{I_{ij}}$ is

$$\hat{g}^{I_{ij}}(x,y) = a_k^{I_{ij}}\cos(f_k^{I_{ij}}(x\cos(d_k^{I_{ij}}) + y\sin(d_k^{I_{ij}})) - ph_k^{I_{ij}}). \tag{2}$$

In our experiment, the following parameters were used: $N_x = N_y = 512 pixel$(scan resolution is $20 pixel/mm$): $M = 8$: $L = 64$: $\sigma = 10$: $K = 5$.

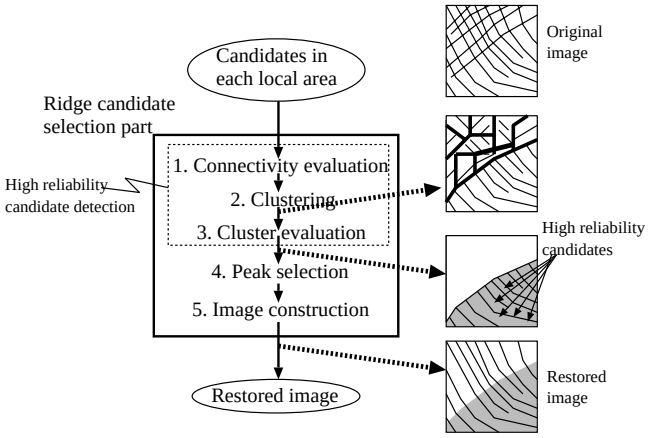

Figure 5. Block diagram of ridge candidate selection part

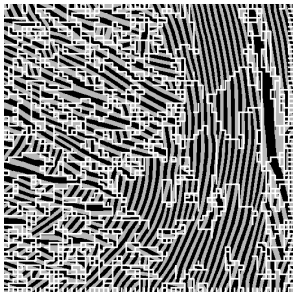

Figure 6. Restored image constructed from 1st candidates and connectivity evaluation result

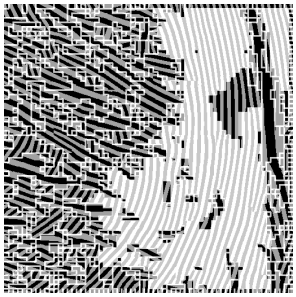

Figure 7. Restored image constructed from 1st candidates and cluster estimation result

To take an example, Fig.3 shows the local image, the power spectrum of which is shown in Fig.4. As the

figure shows, the peaks which correspond to a ridge and a crease are clearly visible.

4. Ridge candidate selection part

4.1. Overview

In the ridge candidate selection part, the candidates originating in the ridges are selected from the candidates detected in the ridge candidate extraction part in each local area, and a restored image(ridge image) is constructed. In this part, at first, candidates with a high probability of being ridges are detected in some local areas. We call such candidates "high reliability candidates" and areas containing such a candidate "high reliability areas". Then, the candidates having high continuity with high reliability candidates are selected in the other areas. The block diagram of ridge candidates selection part is shown in Fig.5.

For detecting high reliability candidates, the likelihood that the 1st candidate is a ridge is evaluated in each local area, and high reliability candidates are detected from among them. Since the 1st candidate has the largest amplitude in its local area, it has the highest likelihood of being a ridge according to local information alone. The groups of local areas whose local information of the 1st candidate varies continuously are then detected(step1 and 2 in Fig. 5). The local information of ridge lines as well as creases varies continuously, but the local information of ridges generally does not have continuity with that of creases. Thus, the 1st candidates in the local area included in each group are all ridges or all creases. Hence the evaluation on whether the 1st candidates are ridges or creases is done for each group (using global information), and several groups are selected(step3 in Fig.5). Then the 1st candidates in the selected group are determined to be high reliability candidates. In our method, for making the groups of local areas, the connectivity of the 1st candidate between a pair of neighboring local areas is evaluated and clusters which have a high degree of continuity are made. All clusters are then evaluated and "high reliability clusters" forming high reliability areas are determined.

Using high reliability candidates detected in this way, candidates corresponding to ridges are selected in other local areas, according to their degree of local information continuity with high reliability candidates(step4 in Fig.5). Finally the ridge image is constructed from the selected candidates(step5 in Fig.5).

Next, let us describe the procedures for each steps of these.

4.2. Connectivity evaluation

In this step, the connectivity of 1st candidates in adjacent (4-neighbor) local areas is evaluated and decisions whether connectivity is good or not are made for each local area. The features used in order to evaluate connectivity are as follows:
(1) the difference in the directions of 1st candidates in each adjacent local area:

$$J_{dir} \equiv |(|d_1^{I_{ij}} - d_1^{I_{neighbor}}| + \frac{\pi}{2}) mod\ \pi - \frac{\pi}{2}|.$$

(2) the difference in the pitches of 1st candidates in each adjacent local area:

$$J_{pitch} \equiv \left| \frac{1}{f_1^{I_{ij}}} - \frac{1}{f_1^{I_{neighbor}}} \right|.$$

(3) the difference in the phase of 1st candidates in each adjacent local area. When the phase of different local areas are compared, these values must be converted into one of their coordinate systems. The translations are as follows.

$$t_{ij}(ph_n^{I_{i+1j}}) = (ph_n^{I_{i+1j}} - 2\pi M f_n^{I_{i+1j}} \cos(d_n^{I_{i+1j}}) + \pi) \quad mod\ 2\pi - \pi \tag{3}$$

$$t_{ij}(ph_n^{I_{ij+1}}) = (ph_n^{I_{ij+1}} - 2\pi M f_n^{I_{ij+1}} \sin(d_n^{I_{ij+1}}) + \pi) \quad mod\ 2\pi - \pi. \tag{4}$$

Hence the difference is defined as:

$$J_{ph} \equiv |(ph_1^{I_{ij}} - t_{ij}(ph_1^{I_{i+1j}}) + \pi) mod\ 2\pi - \pi|.$$

The connectivity of the local area is evaluated as follows:

$$if(J_{dir} < TH_{dir}^L) and (J_{pitch} < TH_{pitch}^L) \\ and (J_{phase} < TH_{phase}^L) \rightarrow Connected \\ Otherwise \rightarrow Not\ connected \quad .$$

TH_{dir}^L, TH_{pitch}^L, and TH_{phase}^L are thresholds.

Let us consider an example. Fig.6 is a composite image which was reconstructed from 1st candidates in each of the local areas by using equation(2) and the connectivity evaluation result obtained using the proposed method. In this image, the bright boundaries between adjacent local areas indicate that they are not connected.

4.3. Clustering

In this step, the local areas whose 1st candidates are determined to be connected in the connectivity evaluation are clustered. The local areas surrounded by the border of the image and the boundaries determined to be "Not connected" are detected, and local area groups are generated by such local areas.

4.4. Cluster evaluation

In this step, the likelihood that the 1st candidate in local areas included in each local area group is a ridge is evaluated. In addition, local area groups with a high likelihood of being ridge lines are determined. We call such a local area group a "high reliability cluster". The likelihood of being a ridge line in each local area group is evaluated with the following features:
(1) The number of local areas included in a local area group. The number of local areas in the ℓ-th local area group is described as N_ℓ
(2) The ratio of the energy of a candidate included in a local area included in the group to the total energy of the local area, which is $Rc_\ell \equiv \frac{\sum_{(i,j)\in C_\ell} va_1^{I_{ij}}}{\sum_{(i,j)\in C_\ell} v_T^{I_{ij}}}$ $(k = 1, \cdots, N)$ where $C_\ell \equiv \{(i,j)|I_{ij} \in \ell th\ local\ area\ group\}$.

The reason we chose to use these features is as follows. In areas including both creases and ridges, it is not clear whether the 1st candidate(i.e. the one having the largest amplitude in a local area) is a crease or a ridge. Since creases and ridges are not connected, the size of the local area group, obtained by the clustering step according to the connectivity of the 1st candidate, does not become large. On the other hand, in a portion in which a ridge line is clearly present without creases, the ridge line becomes the 1st candidate. Thus, the size of the local area group becomes large. The Rc_ℓ of such an area tends to be larger than that of a local area including both ridges and creases.

Local area groups are then evaluated using these features. The procedure consists of two stages:
Cluster evaluation:
Step1. The local area group which satisfies $N_{\ell_0} = max_\ell\{N_\ell\}$ is determined as the high reliability cluster.
Step2. Local area groups which satisfy $Rc_\ell \geq TH_R^C$ and $N_\ell \geq TH_N^C$ are determined as high reliability cluster in the order of N_ℓ to a maximum of 4 (TH_R^C and TH_N^C are thresholds).

An example of the results obtained is shown in Fig.7. In this figure, the bright areas are high reliability clusters(in that their 1st candidates are evaluated as ridges).

4.5. Peak selection

Peak selection is the process for selecting candidate in local areas which are not high reliability areas. Selection is done considering the candidate's own local information and the candidate's connectivity with candidates in the high reliability local areas.

The selecting order of ridge line candidates is as follows. First, selection is done in the local areas adjacent to a high reliability area. When there are no more adjacent to a high reliability areas local areas, selection is done in the local areas adjacent to a local area in which selection has been done. This continues until a selection has been made in all local areas. We use the term "definite candidate" to describe high reliability candidates and the selected candidates included in areas in which the selection step has already been completed. Let u_{ij}-th candidate of local area I_{ij} be a definite candidate. The features used are as follows:
(1) The ratio of the energy of a candidate to the energy of the others:

$$Rp_k^{I_{ij}} \equiv \frac{va_k^{I_{ij}}}{\sum_{n=1}^{6} va_n^{I_{ij}}}$$

(2) The order of candidate k:
(3) Average difference of the candidate phase:

$$D_{ph_k}^{I_{ij}} \equiv \frac{1}{(U_N^{I_{ij}})} \sum_{I_{i'j'}\in U_N^{I_{ij}}} |(t_{ij}(ph_{u_{i'j'}}^{I_{i'j'}}) - ph_k^{I_{ij}} + \pi) mod\ 2\pi - \pi|$$

$U_N^{I_{ij}}$ denotes a set of definite candidates in the areas which are adjacent to local area I_{ij}
(4) Average difference of the candidate direction:

$$D_{d_k}^{I_{ij}} \equiv \frac{1}{(U_S^{I_{ij}})} \sum_{I_{i'j'}\in U_S^{I_{ij}}} |(|d_{u_{i'j'}}^{I_{i'j'}} - d_k^{I_{ij}}| + \frac{\pi}{2}) mod\ \pi - \frac{\pi}{2}|$$

$U_S^{I_{ij}}$ denotes a set of definite candidates in the areas which satisfy $(i-i')^2 + (j-j')^2 \leq S$.

By unifying the these four features, one ridge line candidate is selected for each local area.
Peak selection:
Step1. In a local area from which candidates are to be selected, the candidate of which $D_{d_k}^{I_{ij}}$ is minimized is selected from those that satisfy the following three conditions: 1.$D_{ph_k}^{I_{ij}} < TH_{phase}^P$, 2. $k < TH_N^P$, and 3. $Rp_k^{I_{ij}} > TH_E^P$ (TH_{phase}^P, TH_N^P, and TH_E^P are thresholds).

An example result is shown in Fig.8. This figure is an image obtained by binarizing the images of the candidates sine waves selected in each of the local areas.

4.6. Experimental Result

Fig.9 shows an example of the result obtained with our proposed method. The figure is a thinned image of the original image appearing in Fig.1. For purposes of comparison, a thinned image obtained using a method for fingerprints [3] is shown in Fig.10. Many creases

exist in the left area of the original image(Fig.1). As the figures show, the proposed method is able to extract ridges correctly while avoiding the creases, but the method for fingerprints cannot extract ridges.

4.7. Summary

We have proposed a new method for extracting ridges from palmprint images. Experimental results confirm that the new method's ability to extract ridges in areas including many creases exceeds that of methods for fingerprints.

Acknowledgements

The authors would like to thank the members of the Investigation and Research Committee for Automated Palmprint Identification System in Security Electronics & Communications Technology Association(SECTA) for their valuable comments. We acknowledge Seiji Yoshimoto, Kaoru Uchida, Toshio Kamei and other member of the laboratory staff for their encouragement and advice.

References

[1] K. Asai, Y. Hoshino, Y. Kato, and K. Kiji. Automatic reading and matching for single-fingerprint identification. In *65th International Association for Identification Conference, Ottawa, Canada*, page 17, 1980.

[2] A. Jain and L. Hong. On-line fingerprint verification. In *Proceedings of International Conference on Pattern Recogition*, pages 596–600, 1996.

[3] T. Kamei and M. Mizoguchi. Image filter design for fingerprint enhancement. In *Proceedings of ISCV'95-Florida*, pages 109–114, 1995.

[4] M. Kawagoe and A. Tojo. Fingerprint pattern classification. *Pattern Recognition*, 17(3):295–303, March 1984.

[5] L.O'Gorman and J.V.Nickerson. An approach to fingerprint filter design. *Pattern Recognition*, 22(1):29–38, January 1989.

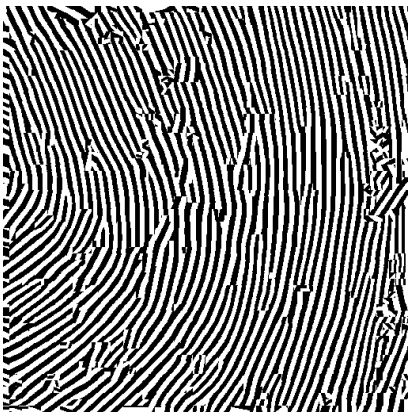

Figure 8. Restored image constructed by the selected candidates

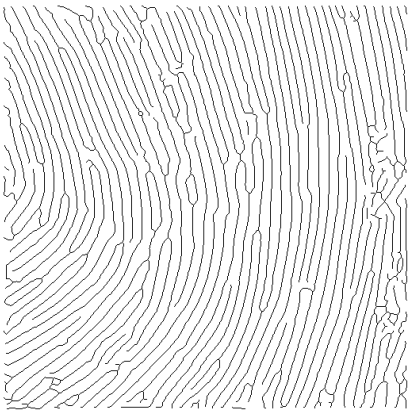

Figure 9. Thinned image obtained with proposed method

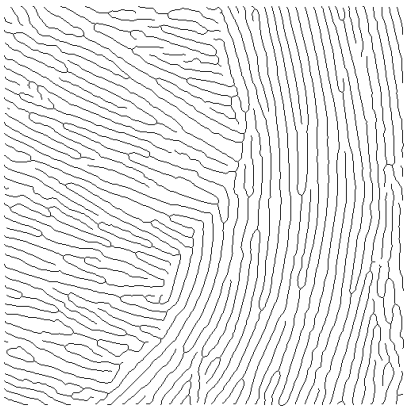

Figure 10. Thinned image obtained with a method for fingerprints[3]